© 2016. Published by The Company of Biologists Ltd | Journal of Cell Science (2016) 129, 3042-3052 doi:10.1242/jcs.183400

RESEARCH ARTICLE

‘Rod and ring’ formation from IMP dehydrogenase is regulated through the one-carbon metabolic pathway

S. John Calise[1], Daniel L. Purich[2], Thuy Nguyen[1], Dania A. Saleem[1], Claire Krueger[1], Joyce D. Yin[1] and Edward K. L. Chan[1,‡]

ABSTRACT

‘Rods and rings’ (RRs) are conserved, non-membrane-bound intracellular polymeric structures composed, in part, of inosine monophosphate dehydrogenase (IMPDH), a key enzyme leading to GMP and GTP biosynthesis. RR formation is induced by IMPDH inhibitors as well as glutamine deprivation. They also form upon treatment of cells with glutamine synthetase inhibitors. We now report that depriving cells of serine and glycine promotes RR formation, and we have traced these effects to dihydrofolate reductase (DHFR) and serine hydroxymethyltransferase-2 (SHMT2), pivotal enzymes in one-carbon metabolism and nucleotide biosynthesis. RR assembly is likewise induced upon DHFR inhibition by methotrexate or aminopterin as well as siRNA-mediated knockdown of DHFR or SHMT2. Because RR assembly occurs when guanine nucleotide biosynthesis is inhibited, and because RRs rapidly disassemble after the addition of guanine nucleotide precursors, RR formation might be an adaptive homeostatic mechanism, allowing IMPDH to sense changes in the one-carbon folate pathway.

KEY WORDS: Allosteric regulation, Cytoophidia, Enzyme inhibition, Enzyme polymerization, Folate metabolism, Intracellular filaments, Nucleotide biosynthesis, One-carbon metabolism

INTRODUCTION

The idea that extensive metabolic changes underlie the unbridled proliferation of cancer cells led Weber (1983) to propose that certain pacemaker enzymes are linked to neoplastic transformation and/or progression, suggesting further that these enzymes should be appropriate targets for chemotherapy. His discovery that inosine 5′-monophosphate dehydrogenase (IMPDH, for which there are two variants, IMPDH1 and IMPDH2, in mammals), which catalyzes the reaction $IMP+H_2O+NAD^+ \rightleftharpoons XMP+NADH+H^+$ and is the rate-limiting enzyme in guanosine monophosphate (GMP) synthesis, is amplified in tumors and rapidly proliferating tissues (Jackson et al., 1975) was an impetus for the development of effective anticancer, immunosuppressive and antiviral chemotherapies (Chen and Pankiewicz, 2007; Nair and Shu, 2007; Ratcliffe, 2006; Shu and Nair, 2008). Later studies showed that, when cells are treated with IMPDH inhibitors or when they are deprived of nutrients required for GMP synthesis, many cells form distinctive structures termed ‘rods and rings’ (RRs), mainly within the cytoplasm (Calise et al., 2014b; Carcamo et al., 2011; Gunter et al., 2008; Ji et al., 2006; Thomas et al., 2012). These macromolecular assemblies take the shape of rods that are typically 3–10 µm in length or rings that most often are 2–5 µm in diameter. Both are composed, at least in part, of IMPDH and/or cytidine triphosphate synthetase (CTPS, which has two variants, CTPS1 and CTPS2, in mammals) (Carcamo et al., 2011; Chang et al., 2015; Keppeke et al., 2015). Those composed mainly of CTPS are named ‘cytoophidia’ or ‘CTPS filaments’ (Ingerson-Mahar et al., 2010; Liu, 2010; Noree et al., 2010). Representing a distinct class of subcellular structures, RRs are not associated with any known organelles or with any of the cytoskeletal proteins (e.g. tubulin, actin and vimentin) (Carcamo et al., 2011; Liu, 2010). Recent reports have demonstrated that RRs form in both the nucleus and cytoplasm (Calise et al., 2014b; Carcamo et al., 2014; Gou et al., 2014).

Initial studies on RR formation focused on RR assembly *in vitro*, mainly by using small-molecule inhibitors targeting IMPDH and CTPS, two allosterically controlled pacemaker enzymes in nucleotide biosynthesis. The conversion of XMP into GMP and that of UTP into CTP require glutamine as a donor of amide nitrogen, relying on their on-board glutaminase activities to mobilize free ammonia. In this respect, RR structures can be effectively induced in any mammalian cell line tested to date by IMPDH inhibitors (mycophenolic acid or ribavirin) or by glutaminase inhibitors [6-diazo-5-oxo-L-norleucine (DON) or acivicin] (Carcamo et al., 2011; Chen et al., 2011; Ji et al., 2006). The glutamine analog azaserine also promotes RR or cytoophidium assembly in both human and *Drosophila* cells (Chen et al., 2011), as do the anti-folate pemetrexed (Carcamo et al., 2014), nucleoside analog decoyinine (Gunter et al., 2008), and the uridine analog deazauridine in mammalian cells (Chang et al., 2015).

Purine and pyrimidine nucleotides are mainly derived from amino acids, and we have demonstrated that depriving cells of glutamine leads to RR formation (Calise et al., 2014b). Moreover, irreversible inhibition of glutamine synthetase by methionine sulfoximine induces RR assembly. An additional study confirmed that both DON inhibition and glutamine deprivation induce cytoophidia assembly in HeLa cells (Gou et al., 2014). That is, without glutamine, nucleotide homeostasis is disturbed, leading to the polymerization of IMPDH and/or CTPS into RRs. Our finding that limiting the supply of particular amino acids induces RR assembly motivated us to examine the impact of other amino acids on this dynamic process. We also found that RR formation occurs when cells are grown in standard culture media (MEM), which lacks serine and glycine, the former a substrate and the latter a product, for serine hydroxymethyltransferase (SHMT, which also has two variants, SHMT1 and SHMT2, in mammals), an enzyme that supplies one-carbon precursors for the C-2 and C-8 atoms within the

[1]Department of Oral Biology, University of Florida, 1395 Center Drive, Gainesville, FL 32610-0424, USA. [2]Department of Biochemistry and Molecular Biology, University of Florida, 1200 Newell Drive, Gainesville, FL 32610-0245, USA.

[‡]Author for correspondence (echan@ufl.edu)

E.K.L.C., 0000-0003-3938-9503

Received 16 November 2015; Accepted 21 June 2016

Journal of Cell Science (2016) 129, 3042-3052 doi:10.1242/jcs.183400

purine ring. The experiments reported here provide new evidence for the interplay of one-carbon folate metabolism with RR formation.

RESULTS

In our earlier study on the effects of glutamine in RR formation, we exclusively used Dulbecco's modified Eagle's medium (DMEM) to culture cells. We later observed, however, that Minimum Essential Medium (MEM) consistently induced RR formation, despite the presence of 2 mM glutamine in this culture medium. Upon comparing the composition of DMEM and MEM, we found that they differ mainly with respect to serine, glycine and $Fe(NO_3)_3$, which are absent in MEM (Table S1). This observation suggested that, even in the presence of adequate glutamine, the absence of serine and glycine might drive RR formation. We note that serine and glycine are also essential for nucleotide biosynthesis (Fig. 1A), with the former required in the synthesis of N^5,N^{10}-methylenetetrahydrofolate (N^5,N^{10}-CH_2-THF) and the latter serving as a direct substrate in the synthesis of glycinamide ribonucleotide (GAR). The differential behavior of DMEM and MEM motivated additional experiments on the effects of serine and glycine deprivation on RR formation. Although the focus here is on RR assembly from IMPDH, work with other antibodies that label CTPS filaments (cytoophidia) did not show CTPS colocalization with RRs formed under conditions used in this study (Fig. S1).

RR formation induced in HeLa and Hep3B cells cultured in MEM

Fig. 1B shows our initial evidence that differences in growth medium composition might explain why RR structures formed in MEM but not DMEM. HeLa cells cultured in standard DMEM did not form RR structures, whereas Hep3B cells grown in standard MEM formed RRs in ~50% of cells (Fig. 1B, left and middle columns). Notably, the size and number of RRs in Hep3B cells in MEM (i.e. serine- and glycine-deficient medium) are similar to that observed for HeLa cells cultured in DMEM lacking glutamine (Fig. 1B, right). Although these data suggested RR assembly is related to differences in DMEM and MEM composition, further

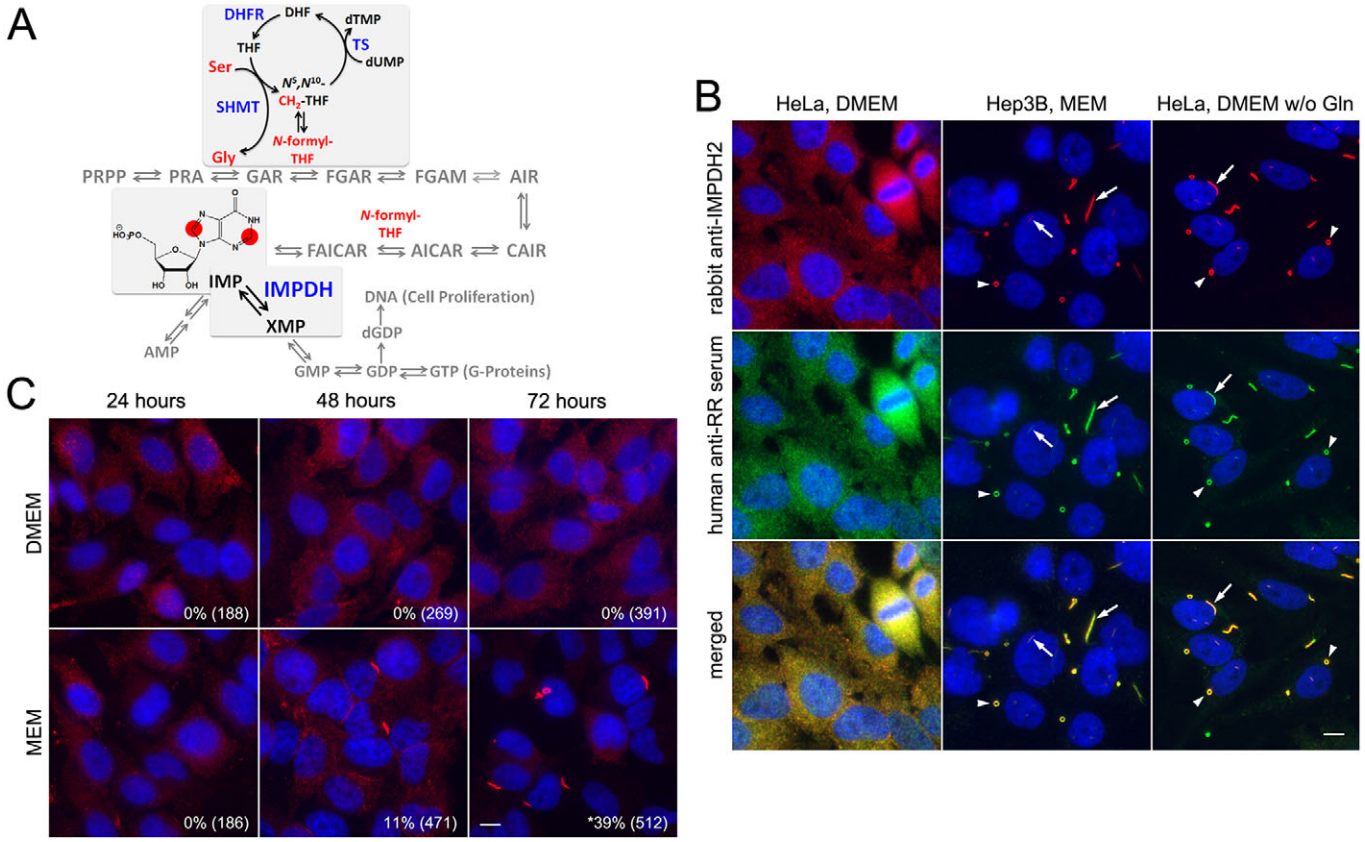

Fig. 1. Differential assembly of RR structures in cells cultured in MEM but not DMEM. (A) Diagram showing interplay of the one-carbon folate pathway (gray box, top) and purine nucleotide biosynthetic pathway (dark gray lettering), demonstrating that N^{10}-formyl-tetrahydrofolate is a key cofactor in both pathways. (Red circles, carbon atoms derived from N^{10}-formyl-THF.) Note that inosine 5′-monophosphate (IMP) lies at a metabolic crossroads leading to adenine and guanine nucleotides. IMPDH catalyzes the NAD^+-dependent oxidation of IMP into xanthosine 5′-monophosphate (XMP), which is subsequently converted into GMP. The latter is also an allosteric feedback inhibitor of IMPDH. GMP is subsequently phosphorylated to form GDP and GTP. Note also that glycine is a direct substrate for glycinamide ribonucleotide (GAR) synthetase and serine is a substrate for serine hydroxymethyltransferase (SHMT). (B) HeLa cells maintained in DMEM did not form RR structures (left), whereas Hep3B cells grown in MEM, which lacks serine, glycine and iron nitrate, presented RRs in ~50% of cells (middle). Additionally, HeLa cells grown in DMEM and then deprived of glutamine for 48 h showed RRs in ~50% of cells (right). Rods (arrows) and rings (arrowheads) appear in cytoplasmic, nuclear and perinuclear regions. (C) HeLa cells cultured in typical DMEM growth medium (top) did not exhibit RRs at various time-points from 24 h to 72 h. HeLa cells cultured in MEM showed RRs as early as 48 h, and maintained these structures after 72 h (bottom). Cells from both groups were first maintained in DMEM and then changed to either DMEM or MEM at time 0 h. The mean percentage of cells positive for RR are shown in the bottom right corner of each image in C, with total number of cells counted for each condition in parentheses. Cells were stained with rabbit anti-IMPDH2 (red) and/or human prototype anti-RR serum It2006 (green); nuclei were counterstained with DAPI (blue). Data shown in panel C are from three independent experiments. *P<0.05 (MEM 72 h versus DMEM 72 h, ANOVA). Scale bars: 10 µm.

Journal of Cell Science (2016) 129, 3042-3052 doi:10.1242/jcs.183400

work was required to define the factor(s) leading to RR formation, and for sake of convenience and self-consistency, all of the findings reported below were carried out with HeLa cells.

We first sought to observe how quickly RR structures formed in HeLa cells initially passaged in DMEM and then transferred to MEM. These cells were cultured in either MEM (test medium) or DMEM (control medium) for 24, 48 or 72 h (Fig. 1C). Those grown in MEM had RR structures in ∼11% of cells by 48 h and ∼39% by 72 h, whereas cells grown in DMEM failed to form RRs at any time-point. (At 96 h, test and control cells appeared comparable to those at 72 h, and no further studies were conducted at the 96-h time-point.) Our results confirmed that RR formation that had been previously observed in Hep3B cells in MEM (Fig. 1B) was unrelated to differences in Hep3B and HeLa cells. Furthermore, although DMEM is a richer growth medium than MEM, which contains lower concentrations of many amino acids, vitamins, and inorganic salts, we decided to focus on serine, glycine and iron nitrate individually first, given that there was a complete lack of these components in MEM (Table S1).

RR formation induced by serine deprivation

HeLa cells were cultured in typical DMEM growth medium and then plated and grown in one of three media: (1) MEM+0.4 mM serine and 0.4 mM glycine added manually (0.4 mM is the standard concentration of these amino acids found in DMEM; Table S1), (2) MEM+0.4 mM glycine, or (3) MEM+0.4 mM serine (Fig. 2A). No RRs were observed over the interval from 0 to 72 h in any cells that had been cultured in MEM when both serine and glycine were included (Fig. 2A, top row). Cells in MEM+0.4 mM glycine formed RRs in a high percentage of cells, ∼52% of cells at 48 h, and ∼88% of cells at 72 h (Fig. 2A, middle row). Cells in MEM with only 0.4 mM serine addition showed virtually no RR formation at any point from time 0 to 72 h (Fig. 2A, bottom row). Strikingly, the presence of serine appeared to prevent RR polymerization, whereas glycine, when alone, promoted RR formation (e.g. ∼52% and ∼88% of cells showing RR at 48 h and 72 h, when lacking only serine, compared to ∼11% at 48 h and ∼39% at 72 h of cells grown in MEM lacking both serine and glycine simultaneously; Fig. 1C).

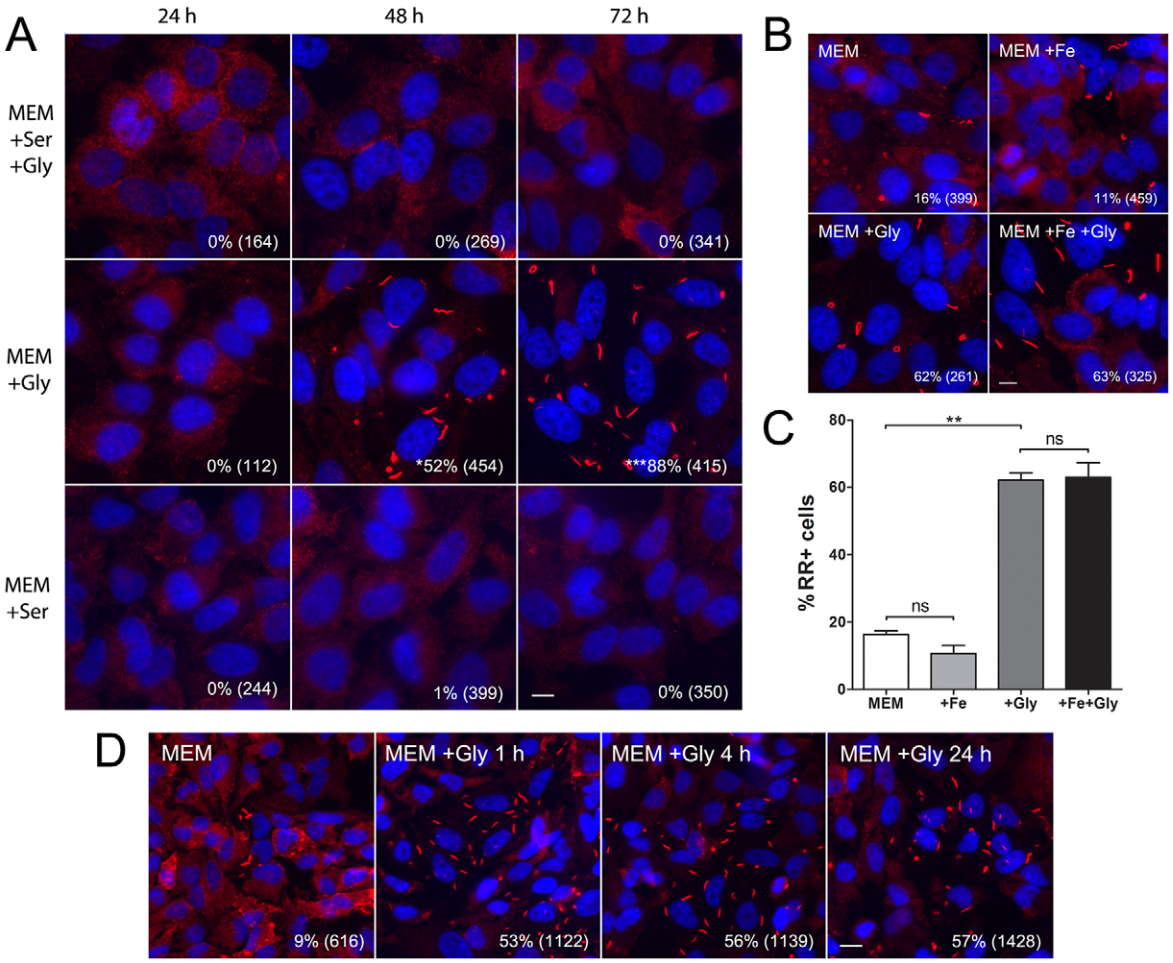

Fig. 2. Serine deprivation induced RR formation and glycine supplementation increased RR formation by 1 h post-treatment. (A) HeLa cells cultured in DMEM were transferred to one of three media: (top) MEM+0.4 mM serine and 0.4 mM glycine, (middle) MEM+0.4 mM glycine, or (bottom) MEM+0.4 mM serine. *P<0.05 (MEM+Gly 48 h versus MEM+Ser+Gly 24 h, ANOVA), ***P<0.001 (MEM+Gly 72 h versus MEM+Ser+Gly 72 h, ANOVA). (B) HeLa cells were cultured for 72 h in MEM, MEM+0.1 mg/l iron nitrate (+Fe) supplement, MEM+0.4 mM glycine supplement (+Gly), or MEM+both (+Fe+Gly). (C) A graphic representation of results from B (mean±s.e.m.). **P<0.01 (MEM 72 h versus MEM+Gly 72 h, ANOVA); ns, not significant. (D) HeLa cells were cultured in MEM for 48 h and then supplemented with glycine for 1 h, 4 h or 24 h. Untreated control cells were left in MEM for 72 h and then fixed simultaneously with other cells. The results show that a particular cell population (∼53–57%) appears more sensitive to glycine supplementation than other cells, but the reasons for this difference are unclear. Cells were stained with rabbit anti-IMPDH2 (red); nuclei were counterstained with DAPI (blue). Scale bars: 10 µm (A,B); 20 µm (D). The mean percentage of cells positive for RRs are shown in the bottom right corner of each image. Data shown in A–C are from three independent experiments; data in D are from two independent experiments.

Journal of Cell Science (2016) 129, 3042-3052 doi:10.1242/jcs.183400

Glycine supplementation promotes RR formation

In view of the unexpected observation that glycine stimulates RR formation when cells are cultured in the absence of serine, we quantified these effects by culturing HeLa cells for 72 h under four different conditions: (1) MEM (which lacks serine, glycine and iron nitrate), (2) MEM supplemented with 0.1 mg/l (<0.001 mM) iron nitrate (as found in DMEM), (3) MEM supplemented with 0.4 mM glycine, or (4) MEM supplemented with both iron nitrate and glycine. We found that RRs were induced in all of these conditions, but there was no significant difference between RR formation in cells cultured in MEM with or without iron nitrate (Fig. 2B,C). Additionally, no significant difference was observed in RR formation between cells cultured in MEM+glycine and cells in MEM+glycine+iron nitrate (Fig. 2B,C). These two observations rule out that iron nitrate affects RR formation. We were, however, struck by the observation that growth in MEM+glycine resulted in the formation of RR in 62–63% of cells compared to only 11–16% for cells grown in MEM minus glycine. It should also be noted that the RR assembly observed in serine-deprived cells with or without glycine was not associated with change in IMPDH protein levels over the 48–72 h timescale required for polymer formation (Fig. S2). Given the potent activation of RR formation by glycine, we decided to examine the timecourse of RR formation in cells cultured in MEM +glycine for much shorter periods than 72 h. After first incubating cells in MEM for 48 h, we observed RR formation in as little as 1 h after addition of glycine alone (i.e. no serine) (Fig. 2D).

Inhibitors targeting dihydrofolate reductase induce RR formation

Having established the impact of serine and glycine levels on the induction of RR formation, we began to consider how and why these two amino acids might so severely impact upon the metabolic response of RR polymerization. The one-carbon metabolic pathway enzyme SHMT catalyzes the conversion of serine to glycine and tetrahydrofolate (THF) to N^5,N^{10}-CH_2-THF. Subsequently, N^5,N^{10}-CH_2-THF acts as a carbon donor in the reaction catalyzed by thymidylate synthase (TYMS), which converts deoxyuridine monophosphate (dUMP) into deoxythymidine monophosphate (dTMP). We previously reported that we could induce RR formation *in vitro* using a 24-h treatment of 10 µM pemetrexed (Carcamo et al., 2014), a folate antimetabolite that nonspecifically inhibits the activity of TYMS and dihydrofolate reductase (DHFR), as well as glycinamide ribonucleotide formyltransferase and aminoimidazole carboxamide ribonucleotide formyltransferase. With the knowledge that serine and glycine levels appear to be crucial in the control of RR formation and that their conversion catalyzed by SHMT also plays an important role in one-carbon metabolism, we sought to determine whether the induction of RR upon pemetrexed treatment was due to its inhibitory activity on dTMP synthesis or purine synthesis. First, to evaluate the impact of DHFR activity on RR assembly, we used two well-known DHFR inhibitors, methotrexate (MTX) and aminopterin (AMT). An in-depth examination of the kinetics of RR induction by MTX and AMT treatment was performed, using concentrations of either inhibitor ranging from 10 µM (pharmacological range) down to 5 nM (K_i range) for times ranging from 30 min to 24 h (Fig. 3A–C). At 10 µM and 1 µM MTX, we observed significant formation of RR by 1 h after treatment, whereas cells treated with 25–100 nM MTX did not form RRs until much later. With AMT, a higher-affinity DHFR inhibitor, RR assembly was noted earlier than with MTX. HeLa cells treated with high-dose MTX (10 µM and 1 µM) were binned into three groups: cells with no RRs, cells with one or two RR structures, and cells with three or more RRs (Fig. 3D,E). For high-dose MTX, the proportion of cells containing only one or two RRs increases over time. One explanation for this behavior is that at earlier time-points, a number of short, structurally unstable RRs form in cells (Fig. 3A, arrowheads), which either aggregate together to form larger mature RRs or undergo polymer length redistribution to favor larger, more stable structures (Fig. 3A, arrows) at later time-points, thereby lowering the total number of RRs per cell. Similar behavior has been reported for cytoskeletal proteins obeying Oosawa-type condensation equilibrium models for linear polymer assembly–disassembly (Kristofferson and Purich, 1981). A prior report has shown that smaller RR structures can assemble together into larger, mature RRs using time-lapse microscopy of HeLa cells expressing HA–IMPDH2–GFP that were treated with mycophenolic acid or decoyinine (Thomas et al., 2012).

Serine, guanosine or hypoxanthine reverse RR assembly

In a previous study, we have shown that RRs induced by glutamine deprivation subsequently underwent extensive disassembly (often in 15 min) when cells were supplemented with either glutamine or guanosine (Calise et al., 2014b). When cells were deprived of serine (by maintaining them in MEM for 72 h) and then supplemented with either 0.4 mM serine or 1 mM guanosine for 15 min, 1 h or 4 h, we found a significant reduction in the percentage of cells containing RR compared to controls (Fig. 4A; 17% versus 2%, 0%, and 0% for serine; 23% versus 1%, 0%, and 0% for guanosine; $P<0.01$). Note that the effects of guanosine were ribonucleoside specific, as addition of cytidine or uridine did not lead to RR disassembly (Fig. S3). We hypothesized that, if one-carbon folate metabolites prevent RR formation by increasing purine biosynthesis, then guanosine supplementation should reverse or reduce the effects of MTX or AMT on RR formation. To test this idea, cells were simultaneously treated with 1 mM guanosine and 1 µM MTX (Fig. 4B, top row) or 1 mM guanosine+1 µM AMT (Fig. 4C, top row) for 1 h, 4 h or 24 h. At every time-point, we found that the addition of guanosine prevented RR formation by MTX or AMT. Cells were also pre-treated with 1 µM MTX (Fig. 4B, bottom row) or 1 µM AMT (Fig. 4C, bottom row) for 28 h, 24 h or 4 h, and then supplemented with 1 mM guanosine for 1 h, 4 h or 24 h, respectively. In each case, the guanosine disassembled RR structures compared to control cells treated only with MTX or AMT (Fig. 4B,C, representative control images of 28 h MTX or AMT treatments). These results suggest that the restoration of GTP levels is a prominent factor in regulating RR assembly and disassembly; although MTX and AMT directly inhibited DHFR, the restoration of GTP levels through guanosine addition readily reversed RR formation.

As a further test of the above hypothesis, we examined the impact of hypoxanthine (HXT) on MTX- and AMT-induced formation of RR structures. In the salvage pathway, HXT is converted into IMP through the action of HXT-guanine phosphoribosyltransferase (HGPRT, also known as HPRT1), with IMP serving as a GMP precursor in the IMPDH and GMP synthase reactions. In this respect, HXT supplementation should alleviate the effect of the antifolates MTX and AMT on purine metabolism. Indeed, we found that HXT supplementation reversed RR formation in (1) cells pre-treated with MTX or AMT for 24 h (Fig. 5, second column, termed ‘HXT reversal’), (2) cells cultured in the simultaneous presence of HXT and MTX or AMT for 24 h (Fig. 5, third column, termed ‘HXT prevention’), or (3) cells pre-treated with HXT for 24 h before treatment with MTX or AMT (Fig. 5, right-most column, termed ‘HXT priming’). Notably, HXT effectively prevented RR assembly

Journal of Cell Science (2016) 129, 3042-3052 doi:10.1242/jcs.183400

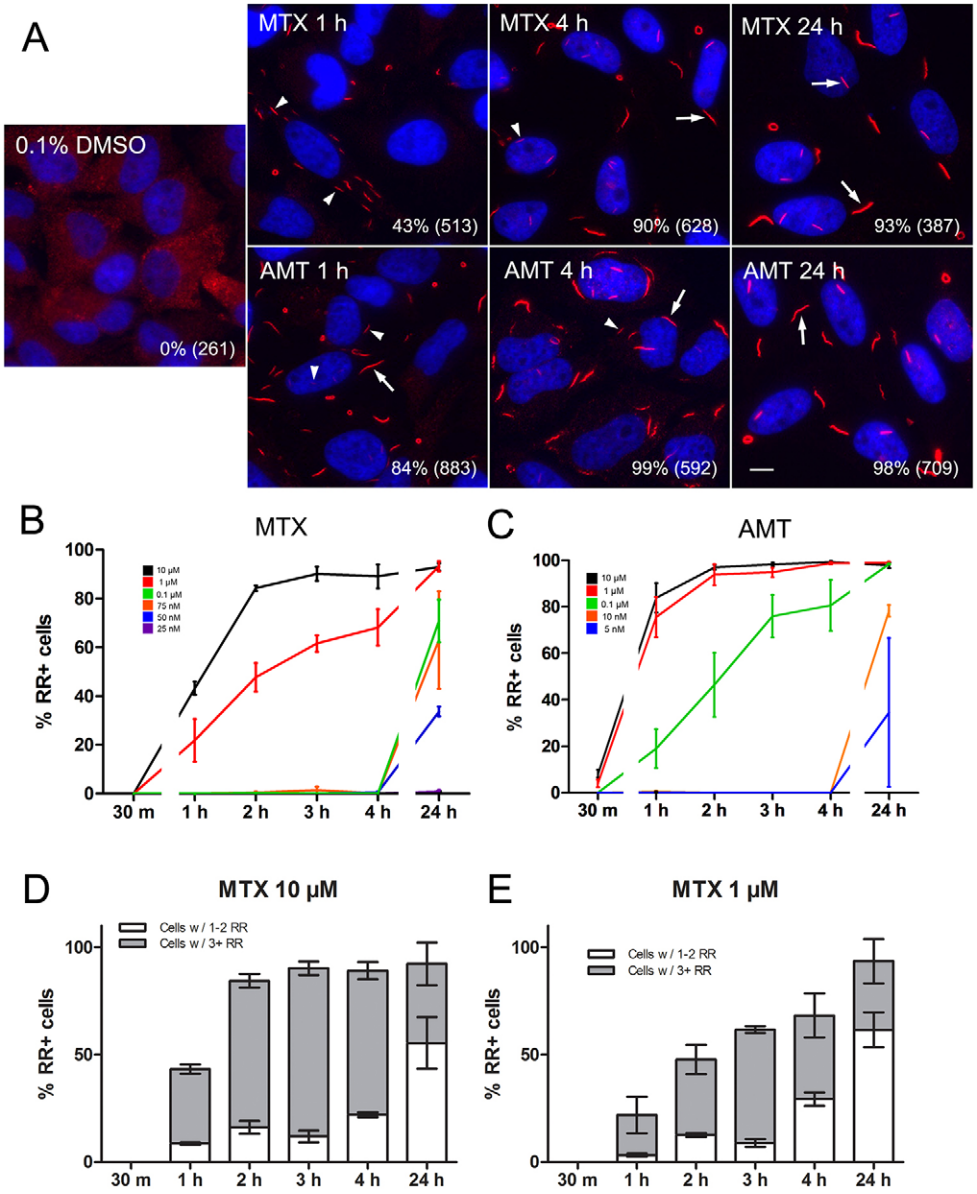

Fig. 3. RR formation is promoted by MTX or AMT in a dose- and time-dependent manner. (A–C) HeLa cells cultured in DMEM were treated with either MTX or AMT at concentrations ranging from 10 μM down to 5 nM for times ranging from 30 min to 24 h. High concentrations of methotrexate (10 μM and 1 μM) caused significant induction of RRs beginning 1 h after treatment, whereas lower concentrations from 0.1 μM down to 50 nM did not induce RRs until after 24 h. (A) Representative images of MTX and AMT treatments, at 1, 4 and 24 h. Immature forms of RRs (arrowheads) might aggregate together to form larger mature RRs (arrows) over time. Cells were stained with rabbit anti-IMPDH2 (red); nuclei were counterstained with DAPI (blue). Scale bar: 10 μm. The mean percentage of cells positive for RRs are shown in the bottom right corner of each image. (B,C) Left axes represent the percentage of treated cells that contained at least one mature rod or ring structure at the time-point measured. Data are from three independent experiments. (D,E) HeLa cells treated with a high dose of MTX (10 or 1 μM) were quantified into separate bins representing no RR induction, one or two mature RRs per cell, or three or more mature RRs per cell. The percentage of treated cells presenting at least one mature RR structure (left axis) is shown further divided into cells with one or two mature RR (white portion of bar) or cells with three or more mature RR (gray portion of bar). Error bars display s.e.m.

in all three cases, when tested with MTX or AMT. However, HXT could not prevent RR assembly in cells treated with the direct IMPDH inhibitors ribavirin and mycophenolic acid. Taken together, these data show that HXT restores guanine nucleotides in MTX- or AMT-treated cells, accompanied by complete disassembly of RRs; however, inhibition of IMPDH in cells treated with ribavirin and mycophenolic acid blocks guanine nucleotide production, no matter the IMP level within the cell. These results provide further evidence that restoration of guanine nucleotides prevents RR formation.

Knockdown of SHMT2 or DHFR induces RR formation

After observing robust RR assembly upon treatment with DHFR inhibitors, we wished to examine whether similar effects could be observed by knocking down the biosynthesis of SHMT, the enzyme catalyzing the conversion of THF (generated by the DHFR reaction) into N^5,N^{10}-CH_2-THF. After overnight culturing in either DMEM (Fig. 6A, top row) or MEM (Fig. 6A, bottom row), HeLa cells were transfected with siRNA targeting SHMT2 (si-SHMT2) or mock-transfected (transfection reagent with no siRNA). Cells cultured in DMEM before and after mock or siRNA transfection did not show any evidence of RRs at 72 h post-transfection, whereas cells cultured in MEM with mock transfection showed RRs in 15% of cells, as would be expected in cells exposed to MEM for 72 h. However, cells cultured in MEM transfected with si-SHMT2 showed a significantly higher percentage of cells containing RRs (Fig. 6B; 71% versus 15%; $P<0.001$). Targeted knockdown of SHMT1 through siRNA was inefficient and did not produce the same results. Both single and pooled siRNA reagents were used, but very minimal knockdown was achieved (data not shown). Several groups have shown that SHMT2 catalysis is responsible for the preponderance of cellular glycine production, with SHMT1 making a smaller contribution (Jain et al., 2012; Kim et al., 2015; Narkewicz et al., 1996). Thus, SHMT2 is the relevant target in our experimental system. These results show that SHMT2 knockdown is not sufficient to induce RR formation in HeLa cells cultured in the nutrient-rich DMEM, but that SHMT2 knockdown exerts an additive effect, increasing the percentage of RR-containing cells in MEM, which lacks serine and glycine.

As an additional test of the methotrexate and aminopterin effects reported above, HeLa cells were cultured overnight in either DMEM

Journal of Cell Science (2016) 129, 3042-3052 doi:10.1242/jcs.183400

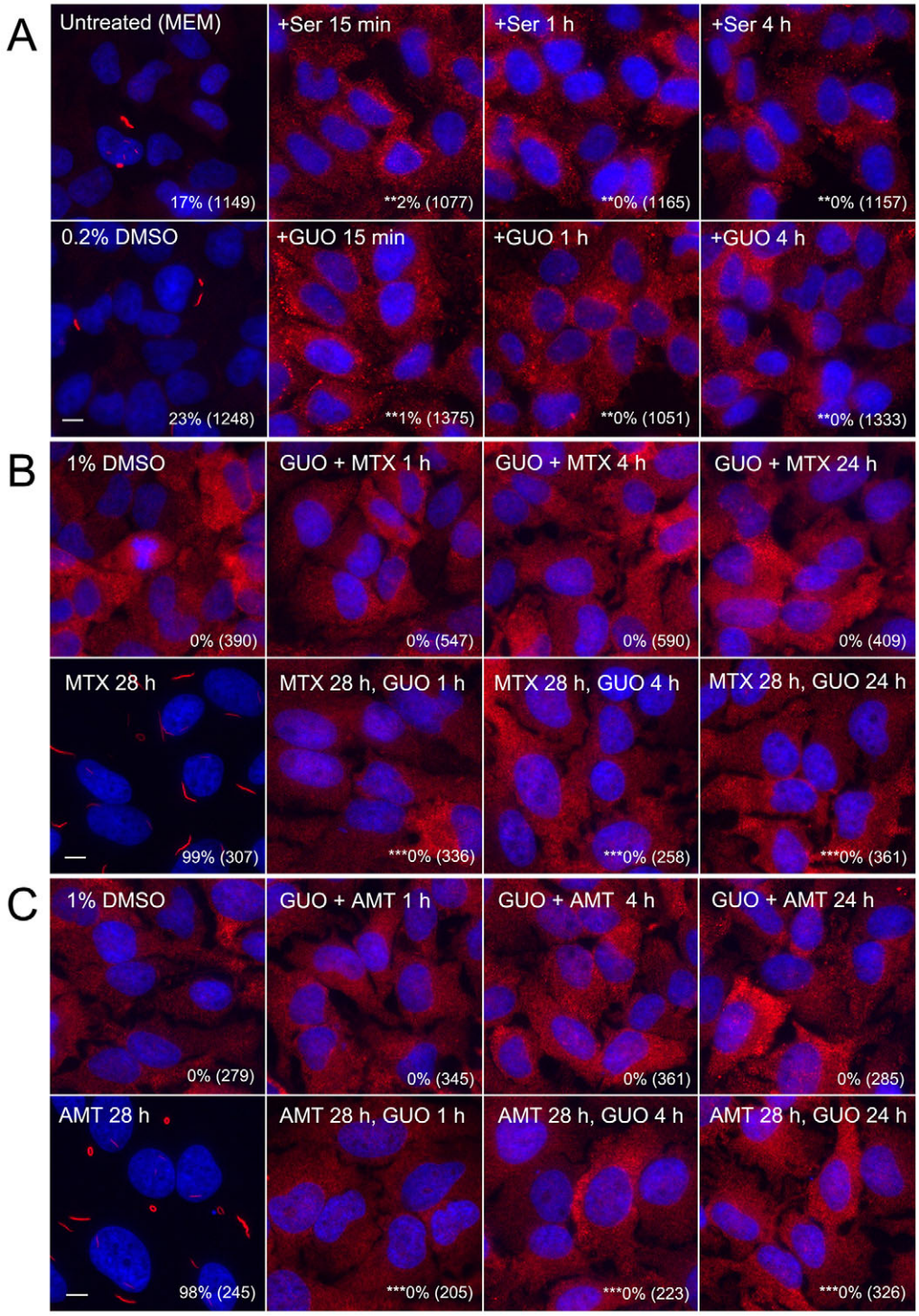

Fig. 4. Serine or guanosine addition prevents or reverses RR assembly caused by serine deprivation, MTX or AMT. (A) HeLa cells were cultured in MEM for 72 h to induce RR formation and then treated with either 0.4 mM serine or 1 mM guanosine (GUO) for 15 min, 1 h, or 4 h. 0.2% DMSO represents a vehicle control for GUO. $^{**}P<0.01$ (MEM+Ser 15 min, +Ser 1 h, +Ser 4 h versus Untreated (MEM); MEM+GUO 15 min, +GUO 1 h, +GUO 4 h versus MEM+0.2% DMSO; ANOVA). (B) HeLa cells cultured in DMEM were either treated with 1 mM GUO and 1 µM MTX simultaneously for 1, 4 or 24 h (top row), or cells were pre-treated with 1 µM MTX for 28, 24 or 4 h and then supplemented with GUO for 1, 4 or 24 h, respectively (bottom row). Total exposure time to MTX was 28 h for cells in bottom row panels, with varying exposure times to GUO such that all cells were fixed simultaneously. $^{***}P<0.001$ (MTX 28 h +GUO 1 h, +GUO 4 h, +GUO 24 h versus MTX 28 h, ANOVA). (C) The same experiment was performed as described in B, except with 1 µM AMT instead of MTX. Cells were stained with rabbit anti-IMPDH2 (red); nuclei were counterstained with DAPI (blue). $^{***}P<0.001$ (AMT 28 h +GUO 1 h, +GUO 4 h, +GUO 24 h versus AMT 28 h, ANOVA). Scale bars: 10 µm. The mean percentage of cells positive for RRs are shown in the bottom right corner of each image. Data in all panels are from three independent experiments.

or MEM and then transfected with siRNA targeting DHFR (si-DHFR) or mock-transfected. Cells cultured in DMEM, before and after a mock transfection, did not form RR at 72 h post-transfection (Fig. 6D). However, cells in DMEM transfected with si-DHFR showed RR formation in 44% of cells at 72 h post-transfection. Cells cultured in MEM with mock transfection displayed RRs in a typical 16% of cells; when cells in the same culture conditions were transfected with si-DHFR, 78% of cells formed RRs at 72 h after transfection. Overall, cells transfected with si-DHFR regardless of culture medium had statistically significant increases in RR formation compared to mock controls (Fig. 6E; 44% versus 0% in DMEM, 78% versus 16% in MEM; $P<0.05$ and $P<0.01$, respectively). An additional positive control for siRNA targeting Lamin A/C (LMNA) demonstrated the specificity of the effects of SHMT2 and DHFR knockdown on RR formation (Fig. S4).

Finally, having evaluated the impact of two of the three enzymes in the dTMP synthetic pathway, we opted to test the effect of thymidylate synthase using the well-known inhibitor 5-fluorouracil (5-FU). Treatment of HeLa cells with 5-FU over the 1 nM–100 µM range for 2 h to 48 h was completely without effect on RR formation in either DMEM or MEM (Fig. 6G). This finding suggests that a drop in the intracellular dTMP level is not a factor in RR formation

Journal of Cell Science (2016) 129, 3042-3052 doi:10.1242/jcs.183400

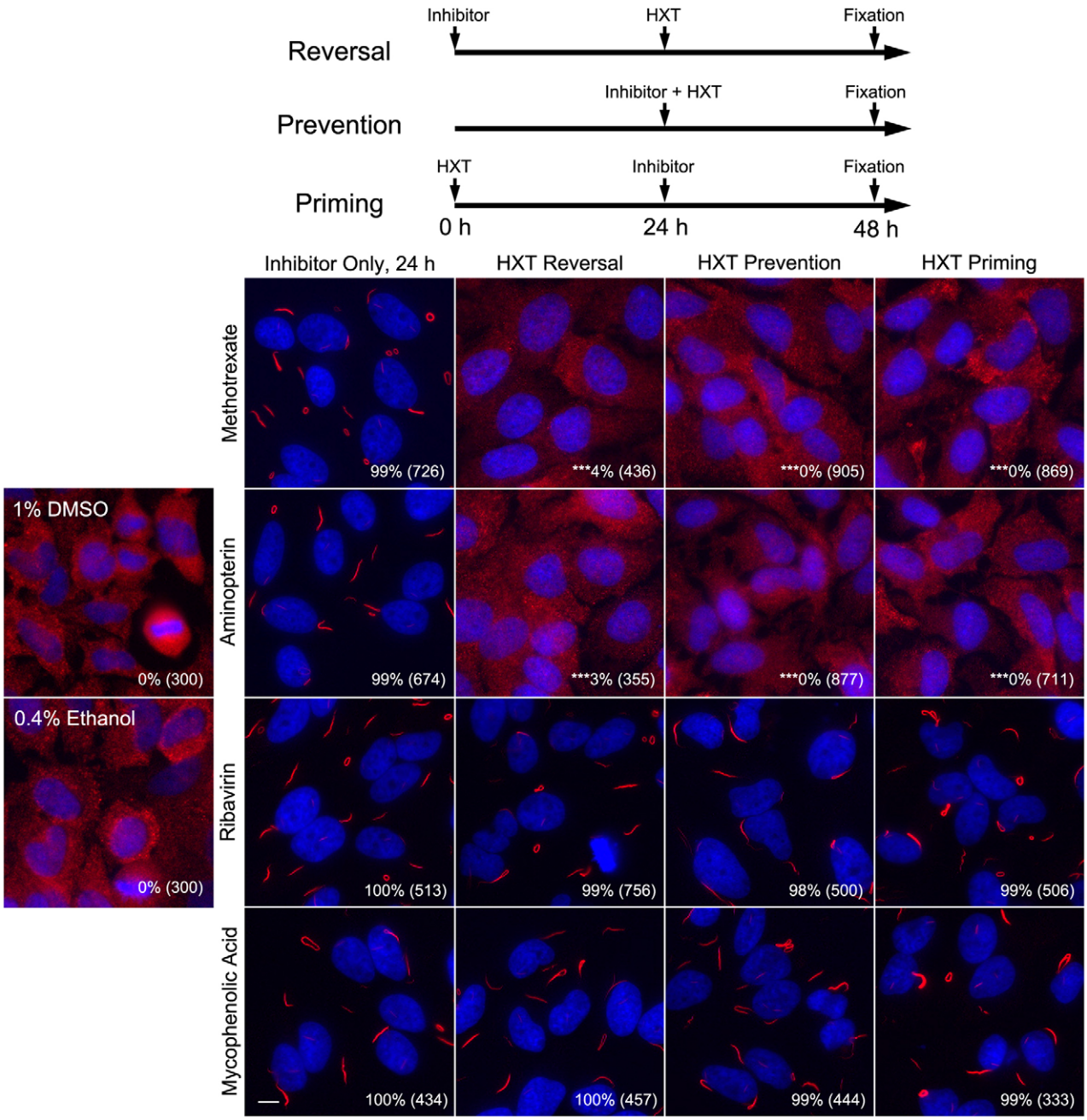

Fig. 5. Addition of HXT prevents or reverses RR assembly induced by MTX or AMT. The effect of HXT was examined using three treatment methods. Reversal, HeLa cells were cultured in DMEM, allowed to attach to a slide, and then treated with one of four inhibitors at time 0 h. DHFR inhibitors MTX and AMT as well as IMPDH inhibitors ribavirin and mycophenolic acid were used. 100 µM HXT was then added to the culture 24 h later with no washing, and incubated for an additional 24 h before fixation. Prevention, HeLa cells were treated with one of four inhibitors plus 100 µM HXT simultaneously, and incubated for 24 h before fixation. Priming, cells were pre-treated with 100 µM HXT at time 0 h for 24 h, and then one of four inhibitors was added without washing, and incubated for an additional 24 h before fixation. 1% DMSO represents vehicle control for MTX and AMT treatments; 0.4% ethanol represents vehicle control for mycophenolic acid treatment. Cells were stained with rabbit anti-IMPDH2 (red); nuclei were counterstained with DAPI (blue). ***P<0.001 (HXT reversal, HXT prevention, HXT priming versus inhibitor-only 24 h for MTX and AMT, ANOVA). The mean percentage of cells positive for RRs are shown in the bottom right corner of each image. Scale bar: 10 µm. Data in all panels are from three independent experiments.

and that depletion of one-carbon folate metabolites promotes RR formation through reduced purine nucleotide biosynthesis.

DISCUSSION

This report provides strong evidence that RR formation from IMPDH is an adaptive mechanism that is stimulated by insufficient serine and excess glycine, as well as RNAi-induced deficiencies in enzymes catalyzing key reactions in one-carbon folate metabolism. Although not a direct substrate for nucleotide biosynthesis, serine provides the methylene moiety for the synthesis of N^5,N^{10}-methylenetetrahydrofolate (N^5,N^{10}-CH_2-THF) in the SHMT reaction. N^5,N^{10}-CH_2-THF plays no direct role in GMP synthesis, but it is essential for dTMP synthesis and is likely to influence the recycling of folate metabolites, thereby affecting the formation of THF and N^{10}-formyl-THF, cofactors that are crucially important in purine nucleotide biosynthesis. The latter supplies two of the six

Journal of Cell Science (2016) 129, 3042-3052 doi:10.1242/jcs.183400

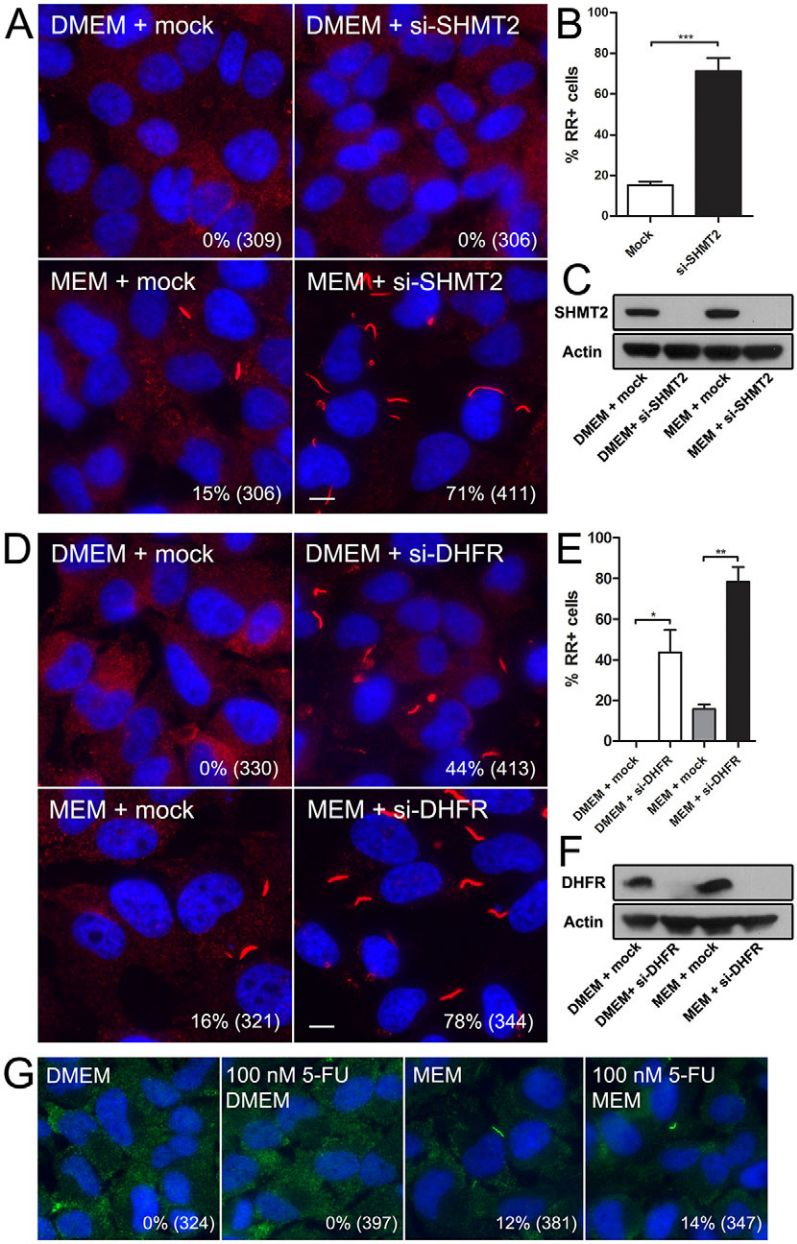

Fig. 6. siRNA knockdown of SHMT2 or DHFR led to increased RR formation. (A) HeLa cells were cultured overnight in either DMEM (top) or MEM (bottom) and then transfected with siRNA targeting SHMT2 (si-SHMT2) or mock-transfected with vehicle excluding siRNA. (B) A graphic representation of data from A. Error bars display s.e.m. ***P<0.001 (MEM+si-SHMT2 vs MEM+mock, two-tailed Student's t-test). (C) Western blot with anti-SHMT2 antibody showing efficient knockdown of SHMT2 protein with siRNA; actin was used as a loading control. (D) HeLa cells were cultured overnight in either DMEM (top row) or MEM (bottom row) and then transfected with siRNA targeting DHFR (si-DHFR) or mock-transfected with vehicle excluding siRNA. (E) Cells transfected with si-DHFR had statistically significant increases in RR formation compared to mock controls (44% vs 0% in DMEM, 78% vs 16% in MEM). Error bars display s.e.m. *P<0.05, **P<0.01 (two-tailed Student's t-test). (F) Western blot with anti-DHFR antibody showing efficient knockdown of DHFR protein with siRNA; actin was used as a loading control. (G) Cells were treated with thymidylate synthase inhibitor 5-FU at concentrations ranging from 1 nM up to 100 µM for 2 to 48 h. 5-FU had no effect on RR formation in DMEM or MEM under any conditions. Representative images of 100 nM 5-FU treatment for 24 h are shown in both DMEM and MEM. Cells were stained with rabbit anti-IMPDH2 (red) or human prototype anti-RR serum It2006 (green); nuclei were counterstained with DAPI (blue). Scale bars: 10 µm. The mean percentage of cells positive for RRs are shown in the bottom right corner of each image. Data in A and B are from four independent experiments; data from D and E are from three independent experiments; data in G represent six independent experiments using various time-points and concentrations of 5-FU.

carbons found in every purine ring (red circles in Fig. 1A). SHMT also forms glycine, itself a direct substrate in *de novo* purine nucleotide biosynthesis.

An emerging theme in RR research is that drugs that throttle GMP biosynthesis, either by directly inhibiting IMPDH (with mycophenolic acid or ribavirin) or indirectly by limiting essential precursor availability (by inhibiting glutamine synthetase with DON or methionine sulfoximine) likewise promote RR assembly (Calise et al., 2014b; Carcamo et al., 2011; Gou et al., 2014; Gunter et al., 2008; Ji et al., 2006). We demonstrated here that RR formation also occurs when cells are treated with methotrexate or aminopterin, which target dihydrofolate reductase. The latter is a crucially important enzyme in folate metabolism and cell survival and proliferation. These drugs are highly effective in promoting RR assembly at pharmacological doses, suggesting that RRs are likely to be found in tissues of patients receiving antifolates during cancer chemotherapy (e.g. the Methotrexate Leucovorin Rescue protocol) and during immunosuppression for rheumatoid arthritis. We and others have demonstrated an autoantibody response against RR structures (IMPDH as a major autoantigen) in a subset of hepatitis C patients that have undergone interferon-α and ribavirin therapy (Carcamo et al., 2013; Covini et al., 2012; Keppeke et al., 2012). Prolonged exposure to interferon-α and ribavirin increases the prevalence of this autoantibody response (Keppeke et al., 2014), and in rare cases anti-RR antibody can be detected in non-hepatitis patients (Calise et al., 2014a, 2015). Such considerations point to the need to investigate the roles of chemotherapeutic agents that might regulate the rate and extent of IMPDH assembly into RR structures.

It is worth noting that SHMT catalyzes the reversible conversion of serine and THF into glycine and N^5,N^{10}-CH_2-THF (Girgis et al., 1998). Intriguingly, excess glycine is not only a product inhibitor, because SHMT also catalyzes a second reaction, namely the irreversible conversion of N^5,N^{10}-CH_2-THF into N^5-formyl-THF (Stover and Schirch, 1993). (The latter must not be confused with N^{10}-formyl-THF, the actual precursor of C-2 and C-8 of the purine

Journal of Cell Science (2016) 129, 3042-3052 doi:10.1242/jcs.183400

ring.) Once synthesized, N^5-formyl-THF remains bound to the enzyme and acts as a slow-binding inhibitor both *in vitro* and *in vivo* (Girgis et al., 1997; Stover and Schirch, 1990). In MCF7 cells, elevated N^5-formyl-THF decreases the biosynthesis of purine nucleotides (Bertrand and Jolivet, 1989), indicating that elevated glycine exerts an inhibitory effect (much like ribavirin, DON and mycophenolic acid) by favoring the formation of N^5-formyl-THF. It follows that the ability of elevated serine to overcome glycine-induced RR formation is explained by the fact that serine and glycine compete for the same amino-acid-binding pocket within the active site of SHMT (Stover and Schirch, 1990, 1993).

Enzyme oligomerization or polymerization is a well-known theme for modulating catalytic activity in response to activators, inhibitors and posttranslational modification (O'Connell et al., 2012; Purich, 2010). In the case of nucleotide biosynthesis, filament formation by IMPDH and CTPS has been studied intensively. In 2010, three research groups independently demonstrated that CTPS assembles into CTPS filaments (Ingerson-Mahar et al., 2010; Noree et al., 2010) or cytoophidia (Liu, 2010) in bacteria, yeast and *Drosophila*. We subsequently demonstrated that, depending on many factors, both CTPS- and IMPDH-containing RR structures can form in mammalian cells (Carcamo et al., 2011; Keppeke et al., 2015). Colocalization of CTPS and IMPDH was inferred by using anti-CTPS1 (kindly provided by Jim Wilhelm, Section on Cell and Developmental Biology, University of California, San Diego, USA), an antibody that is no longer available. Although colocalization of IMPDH and CTPS cannot be demonstrated using commercial antibodies under similar conditions (Calise et al., 2014b), CTPS and IMPDH do colocalize when cells are treated with DON, which irreversibly inhibits CTP and GMP synthases (Chang et al., 2015; Keppeke et al., 2015). As described in Fig. S1, serine deprivation or treatment with MTX or AMT showed no evidence of colocalization.

The present studies also demonstrated the reversibility of RR formation. Upon addition of sufficient HXT or guanosine, which are precursors of IMP and GMP, these structures disassemble rapidly and extensively (Figs 4 and 5). The sensitivity of RR polymerization to guanosine was described previously (Calise et al., 2014b; Gunter et al., 2008; Ji et al., 2006; Thomas et al., 2012), although not in the context of the novel methods used to induce RR in the present study. Significantly, a recent report showed that RRs composed of IMPDH could be induced in CTPS1-overexpressing HEK293T cells, despite no detectable change in GTP levels (Chang et al., 2015). This observation suggests that guanine nucleotide deficiency might not be the only driver of IMPDH assembly into RRs. However, RR formation appears to be exquisitely sensitive to guanine nucleotide levels (through guanosine treatment) under the experimental conditions related to deficiency in one-carbon metabolism used in the current study. Clearly, further studies will be required to characterize other factors, beyond guanine nucleotide levels, that regulate the process of RR formation.

IMP stands at a metabolic crossroad leading to either AMP or GMP. IMPDH catalyzes the first committed step in the eventual synthesis of GMP, GDP and GTP. Given the current understanding of the key roles of G-proteins in cellular homeostasis, it is not surprising that uncontrolled activation of these regulatory proteins can lead to oncogenic transformation. When viewed in the context of Weber's idea that pacemaker enzymes, such as IMPDH, are amplified in tumors and rapidly proliferating cells, it is not surprising that enzymes like IMPDH are endowed with regulatory mechanisms that control their catalytic reaction. RR formation might be a way that cells can increase the amount of enzyme required for GMP synthesis without increasing the concentration of unpolymerized IMPDH. Recent work from the Benkovic laboratory has shown that the enzymes catalyzing early steps of the *de novo* purine nucleotide biosynthesis pathway also assemble to form a dynamic metabolic complex known as the purinosome (Zhao et al., 2013). Like RR formation, purinosome assembly responds to changes in cell culture medium, and purine depletion or 2-dimethylamino-4,5,6,7-tetrabromo-1*H*-benzimidazole (DMAT) treatment stimulates purinosome assembly in HeLa cells. Purinosome formation and dissociation were found to be modulated by several factors, including the microtubule network and cell signaling through protein phosphorylation (Deng et al., 2012). Significantly, although IMPDH itself appears to be a purinosome component, RR and purinosomes were shown to be distinct cellular bodies, which, under favorable conditions, could be simultaneously visualized within the same cells (Zhao et al., 2015). One cannot dismiss the possibility that RRs form when IMPDH levels required by the cell exceed the amount needed to form purinosome complexes.

Further work on RR assembly and disassembly promises to uncover how subunit–subunit interactions promote the formation of these macromolecular structures and how such interactions can be exploited to develop novel anticancer, immunosuppressive and antiviral chemotherapies. Such investigations might also disclose the identity of naturally occurring modulators of RR assembly and disassembly.

MATERIALS AND METHODS

Cell culture

Hep3B cells (human hepatocellular carcinoma; ATCC, Manassas, VA: HB-8064) were cultured in MEM (Mediatech, Inc.: 10-010-CV; or HyClone Laboratories: SH30024.01) supplemented with 10% fetal bovine serum, 100 IU/ml penicillin and 100 µg/ml streptomycin in a 37° incubator containing 5% CO_2. HeLa cells (human cervical adenocarcinoma; ATCC: CCL-2) were cultured in DMEM (Mediatech, Inc.: 10-013-CV; or HyClone Laboratories: SH30243.01) or MEM supplemented with 10% fetal bovine serum, 100 IU/ml penicillin and 100 µg/ml streptomycin under the same conditions. Cell cultures were maintained at 50% confluence. Cell lines were not recently authenticated and tested for contamination.

Indirect immunofluorescence

HeLa or Hep3B cells were cultured in eight-well chambered slides (BD Biosciences: 354108) at a density of ∼50,000 cells per well in 500 µl of medium and used for indirect immunofluorescence assays as previously described (Fritzler et al., 1993; Jakymiw et al., 2006). Cells were fixed with 4% paraformaldehyde in PBS at room temperature for 10 min and then permeabilized with 0.1% Triton X-100 in PBS for 3 min. In experiments involving co-staining of RR structures, cells were labeled with affinity-purified rabbit polyclonal anti-IMPDH2 antibody (Proteintech: 12948-1-AP) and human prototype anti-RR serum It2006 used in previous studies (Carcamo et al., 2011; Covini et al., 2012) at a dilution of 1:500 in PBS, followed by Alexa-Fluor-568-conjugated goat anti-rabbit-IgG (Thermo Fisher Scientific: A11036) and Alexa-Fluor-488-conjugated goat anti-human-IgG (Thermo Fisher Scientific: A11013) secondary antibodies at a dilution of 1:400 in PBS. Additional antibodies used for immunofluorescence in this study include affinity-purified goat polyclonal anti-CTPS1 antibody (Santa Cruz Biotechnology: sc-131474; dilution 1:200), affinity-purified rabbit polyclonal anti-CTPS1 antibody (Proteintech: 15914-1-AP; dilution 1:500), affinity-purified rabbit polyclonal anti-CTPS2 antibody (Proteintech: 12852-1-AP; dilution 1:100), affinity-purified rabbit polyclonal anti-CTPS antibody (GeneTex: GTX105265; dilution 1:100), and human anti-RR serum 608 (dilution 1:200) from a collection of patient sera previously described (Carcamo et al., 2014, 2011; Covini et al., 2012). For co-staining experiments involving goat polyclonal anti-CTPS1 antibody and human anti-RR serum 608, secondary antibodies used were Alexa-Fluor-568-conjugated donkey anti-goat-IgG (Thermo Fisher Scientific: A11057) and DyLight-488-conjugated donkey anti-human-IgG (Thermo Fisher Scientific: SA5-10126), both diluted 1:400 in PBS.

RR formation mediated by serine deprivation and/or glycine supplementation

HeLa or Hep3B cells were cultured in eight-well chambered slides as described above in MEM, which was replaced once daily for the duration of the experiment. As a control, cells were simultaneously cultured in DMEM under what were otherwise the same conditions. After 24 h, 48 h or 72 h, cells were either fixed or treated with glycine (Sigma-Aldrich: G8790), L-serine (Sigma-Aldrich: S4311), iron(III) nitrate nonahydrate (Sigma-Aldrich: F8508), guanosine (Sigma-Aldrich: G6264), HXT (Sigma-Aldrich: H9636), cytidine (Sigma-Aldrich: C4654), or uridine (Sigma-Aldrich: U3003) at designated concentrations ranging from <0.001 mM to 1 mM for varying lengths of time ranging from 15 min to 24 h (indicated on a per-experiment basis within each figure legend). Glycine, L-serine, cytidine and uridine were solubilized in water to a stock concentration of 100 mM. Iron(III) nitrate nonahydrate was solubilized directly in DMEM or MEM to appropriate experimental concentrations. Guanosine and HXT were solubilized in dimethyl sulfoxide (DMSO) to stock concentrations of 100 mM and 50 mM, respectively. Cells shown in Fig. 1C under glutamine deprivation were cultured in DMEM without glutamine (Mediatech, Inc.: 15-013-CV) for 48 h total, with a change of medium at 24 h as previously described (Calise et al., 2014b).

RR formation using DHFR inhibitors or IMPDH inhibitors

Methotrexate (MTX; Sigma-Aldrich: M9929), aminopterin (AMT; Santa Cruz Biotechnology: sc-202461), and 5-fluorouracil (5-FU; Sigma-Aldrich: F6627) were solubilized in DMSO to a stock concentration of 100 mM. Ribavirin (Sigma-Aldrich: R9644) was solubilized in water to a stock concentration of 50 mM. Mycophenolic acid (Sigma-Aldrich: M5255) was solubilized in ethanol to a stock concentration of 31 mM. Cells were seeded in eight-well slides as described above and allowed to adhere to the slide overnight before MTX, AMT, ribavirin or mycophenolic acid were added to the wells at various final concentrations from 25 nM to 100 µM for time-points ranging from 30 min to 24 h (indicated on a per-experiment basis within each figure legend). Guanosine and HXT used to disassemble RRs formed upon inhibitor treatment were prepared in the same manner as described in the previous section.

Induction of RR formation by siRNA knockdown

For the experiments involving siRNA targeting SHMT2, DHFR, SHMT1 or LMNA, all siRNAs were acquired from GE Dharmacon and solubilized in water to a 20 µM stock concentration and stored at −80°C prior to use. Predesigned siRNAs from GE Dharmacon used in this study include siGENOME individual duplex human SHMT2 siRNA (D-004906-01-0002), siGENOME individual duplex human DHFR siRNA (D-008799-03-0002), siGENOME individual duplex human SHMT1 siRNA (D-004617-01-0002), siGENOME SMARTpool SHMT1 siRNA (M-004617-00-0010) and siGENOME individual duplex human LMNA siRNA (D-004978-01-0005). Transfection of siRNA to a final concentration of 100 nM was performed using Lipofectamine 2000 Transfection Reagent (Thermo Fisher Scientific: 11668-019) according to the manufacturer's instructions and as described in our previous studies (Jung et al., 2013, 2012; Lian et al., 2009; Yao et al., 2012, 2011). To ensure success of the transfection, cells were temporarily cultured in Opti-MEM Reduced Serum Medium (Thermo Fisher Scientific: 31985-070) for 6 h during transfection as per manufacturer's instructions, and then switched back to either DMEM or MEM described above for the duration of the experiment. Efficiency of knockdown was analyzed by western blotting using antibodies to SHMT2, DHFR, SHMT1 and LMNA. Antibodies used for western blotting in this study include affinity-purified rabbit polyclonal anti-SHMT2 antibody (Proteintech: 11099-1-AP; dilution 1:800), affinity-purified rabbit polyclonal anti-DHFR antibody (Proteintech: 15194-1-AP; dilution 1:500), affinity-purified rabbit polyclonal anti-SHMT1 antibody (Proteintech: 14149-1-AP; dilution 1:500), mouse monoclonal anti-Lamin A/C antibody (636) (Santa Cruz Biotechnology: sc-7292; dilution 1:100), and mouse monoclonal anti-β-actin antibody (Proteintech: 60008-1-Ig; dilution 1:2000) as a loading control. The procedure for western blotting is briefly described below.

Quantification of IMPDH protein expression by western blot analysis

Cell lysates were prepared using 1% Nonidet P-40 buffer [150 mM NaCl, 50 mM Tris-HCl (pH 8.0), 1% Nonidet P-40] containing Halt Protease Inhibitor Cocktail (Thermo Fisher Scientific: 78430). Protein levels were quantitated using the Pierce BCA Protein Assay Kit (Thermo Fisher Scientific: 23227) and then run on a 12% polyacrylamide gel and transferred to nitrocellulose membrane. Expression of IMPDH and loading control tubulin were detected using an affinity-purified rabbit polyclonal anti-IMPDH2 antibody (Proteintech: 12948-1-AP; dilution 1:1000) and mouse monoclonal anti-α-tubulin antibody (Sigma-Aldrich: T9026; dilution 1:10,000) followed by goat anti-rabbit and goat anti-mouse antibodies conjugated to horseradish peroxidase at 1:5000 dilutions (SouthernBiotech). Immunoreactive bands were detected using the SuperSignal West Pico Chemiluminescent Substrate (Thermo Fisher Scientific: 34080). Expression of IMPDH was quantified and normalized to tubulin expression by densitometric analysis using Fiji or ImageJ software.

Statistical analysis and quantification of RRs

Cell counting, including quantification of the percentage of cells containing RR structures and separation of cells into bins, was performed manually by two or three readers (S.J.C., T.N., D.A.S. and C.K.) per experiment to ensure accuracy of the quantification. Manual counting was performed using the Cell Counter plugin included in Fiji or ImageJ software (Schindelin et al., 2012). With the knowledge that IMPDH localizes to purinosomes as well as RRs (Zhao et al., 2015), only mature filamentous RRs were included in the quantification of the percentage of cells containing RRs. Any foci or short, immature RRs that could not be readily distinguished from purinosomes or other assemblies were not considered RRs. Analysis of variance (ANOVA) or two-tailed Student's *t*-test were used to check for significant differences ($P<0.05$) between independent groups where appropriate. GraphPad Prism 5.0 was used for all statistical analyses.

Acknowledgements

The authors would like to thank Hyun Min Jung (NICHD) for his advice on the technical aspects of the siRNA knockdown experiments and statistical analyses performed in this study.

Competing interests

The authors declare no competing or financial interests.

Author contributions

S.J.C., D.L.P. and E.K.L.C. conceptualized the study. S.J.C. and E.K.L.C. designed the experimental methods used in the study. S.J.C., T.N., D.A.S., C.K. and J.D.Y. performed the experiments. S.J.C., D.L.P. and E.K.L.C. analyzed the data. S.J.C. and D.L.P. wrote the original draft of the manuscript. S.J.C., D.L.P. and E.K.L.C. participated in critical review and editing of the manuscript. All authors read and approved the final manuscript.

Funding

This research received no specific grant from any funding agency in the public, commercial or not-for-profit sectors.

Supplementary information

Supplementary information available online at
http://jcs.biologists.org/lookup/doi/10.1242/jcs.183400.supplemental

References

Bertrand, R. and Jolivet, J. (1989). Methenyltetrahydrofolate synthetase prevents the inhibition of phosphoribosyl 5-aminoimidazole 4-carboxamide ribonucleotide formyltransferase by 5-formyltetrahydrofolate polyglutamates. *J. Biol. Chem.* **264**, 8843-8846.

Calise, S. J., Carcamo, W. C., Ceribelli, A., Dominguez, Y., Satoh, M. Chan, E. K. (2014a). Antibodies to rods and rings. In *Autoantibodies* (ed. Y. Shoenfeld, P. L. Meroni and M. E. Gershwin), pp. 161-168. Elsevier Science.

Calise, S. J., Carcamo, W. C., Krueger, C., Yin, J. D., Purich, D. L. and Chan, E. K. L. (2014b). Glutamine deprivation initiates reversible assembly of mammalian rods and rings. *Cell. Mol. Life Sci.* **71**, 2963-2973.

Calise, S. J., Keppeke, G. D., Andrade, L. E. C. and Chan, E. K. L. (2015). Anti-rods/rings: a human model of drug-induced autoantibody generation. *Front. Immunol.* **6**, 41.

Carcamo, W. C., Satoh, M., Kasahara, H., Terada, N., Hamazaki, T., Chan, J. Y. F., Yao, B., Tamayo, S., Covini, G., von Mühlen, C. A. et al. (2011). Induction of cytoplasmic rods and rings structures by inhibition of the CTP and GTP synthetic pathway in mammalian cells. *PLoS ONE* **6**, e29690.

Carcamo, W. C., Ceribelli, A., Calise, S. J., Krueger, C., Liu, C., Daves, M., Villalta, D., Bizzaro, N., Satoh, M. and Chan, E. K. L. (2013). Differential reactivity to IMPDH2 by anti-rods/rings autoantibodies and unresponsiveness to pegylated interferon-alpha/ribavirin therapy in US and Italian HCV patients. *J. Clin. Immunol.* **33**, 420-426.

Carcamo, W. C., Calise, S. J., von Mühlen, C. A., Satoh, M. and Chan, E. K. L. (2014). Molecular cell biology and immunobiology of mammalian rod/ring structures. *Int. Rev. Cell Mol. Biol.* **308**, 35-74.

Chang, C.-C., Lin, W.-C., Pai, L.-M., Lee, H.-S., Wu, S.-C., Ding, S.-T., Liu, J.-L. and Sung, L.-Y. (2015). Cytoophidium assembly reflects upregulation of IMPDH activity. *J. Cell Sci.* **128**, 3550-3555.

Chen, L. and Pankiewicz, K. W. (2007). Recent development of IMP dehydrogenase inhibitors for the treatment of cancer. *Curr. Opin. Drug Discov. Dev.* **10**, 403-412.

Chen, K., Zhang, J., Tastan, O. Y., Deussen, Z. A., Siswick, M. Y.-Y. and Liu, J.-L. (2011). Glutamine analogs promote cytoophidium assembly in human and Drosophila cells. *J. Genet. Genomics* **38**, 391-402.

Covini, G., Carcamo, W. C., Bredi, E., von Mühlen, C. A., Colombo, M. and Chan, E. K. L. (2011). Cytoplasmic rods and rings autoantibodies developed during pegylated interferon and ribavirin therapy in patients with chronic hepatitis C. *Antivir. Ther.* **17**, 805-811.

Deng, Y., Gam, J., French, J. B., Zhao, H., An, S. and Benkovic, S. J. (2012). Mapping protein-protein proximity in the purinosome. *J. Biol. Chem.* **287**, 36201-36207.

Fritzler, M. J., Hamel, J. C., Ochs, R. L. and Chan, E. K. (1993). Molecular characterization of two human autoantigens: unique cDNAs encoding 95- and 160-kD proteins of a putative family in the Golgi complex. *J. Exp. Med.* **178**, 49-62.

Girgis, S., Suh, J. R., Jolivet, J. and Stover, P. J. (1997). 5-Formyltetrahydrofolate regulates homocysteine remethylation in human neuroblastoma. *J. Biol. Chem.* **272**, 4729-4734.

Girgis, S., Nasrallah, I. M., Suh, J. R., Oppenheim, E., Zanetti, K. A., Mastri, M. G. and Stover, P. J. (1998). Molecular cloning, characterization and alternative splicing of the human cytoplasmic serine hydroxymethyltransferase gene. *Gene* **210**, 315-324.

Gou, K.-M., Chang, C.-C., Shen, Q.-J., Sung, L.-Y. and Liu, J.-L. (2014). CTP synthase forms cytoophidia in the cytoplasm and nucleus. *Exp. Cell Res.* **323**, 242-253.

Gunter, J. H., Thomas, E. C., Lengefeld, N., Kruger, S. J., Worton, L., Gardiner, E. M., Jones, A., Barnett, N. L. and Whitehead, J. P. (2008). Characterisation of inosine monophosphate dehydrogenase expression during retinal development: differences between variants and isoforms. *Int. J. Biochem. Cell Biol.* **40**, 1716-1728.

Ingerson-Mahar, M., Briegel, A., Werner, J. N., Jensen, G. J. and Gitai, Z. (2010). The metabolic enzyme CTP synthase forms cytoskeletal filaments. *Nat. Cell Biol.* **12**, 739-746.

Jackson, R. C., Weber, G. and Morris, H. P. (1975). IMP dehydrogenase, an enzyme linked with proliferation and malignancy. *Nature* **256**, 331-333.

Jain, M., Nilsson, R., Sharma, S., Madhusudhan, N., Kitami, T., Souza, A. L., Kafri, R., Kirschner, M. W., Clish, C. B. and Mootha, V. K. (2012). Metabolite profiling identifies a key role for glycine in rapid cancer cell proliferation. *Science* **336**, 1040-1044.

Jakymiw, A., Ikeda, K., Fritzler, M. J., Reeves, W. H., Satoh, M. and Chan, E. K. L. (2006). Autoimmune targeting of key components of RNA interference. *Arthritis Res. Ther.* **8**, R87.

Ji, Y., Gu, J., Makhov, A. M., Griffith, J. D. and Mitchell, B. S. (2006). Regulation of the interaction of inosine monophosphate dehydrogenase with mycophenolic Acid by GTP. *J. Biol. Chem.* **281**, 206-212.

Jung, H. M., Phillips, B. L., Patel, R. S., Cohen, D. M., Jakymiw, A., Kong, W. W., Cheng, J. Q. and Chan, E. K. L. (2012). Keratinization-associated miR-7 and miR-21 regulate tumor suppressor reversion-inducing cysteine-rich protein with kazal motifs (RECK) in oral cancer. *J. Biol. Chem.* **287**, 29261-29272.

Jung, H. M., Patel, R. S., Phillips, B. L., Wang, H., Cohen, D. M., Reinhold, W. C., Chang, L. J., Yang, L. J. and Chan, E. K. (2013). Tumor suppressor miR-375 regulates MYC expression via repression of CIP2A coding sequence through multiple miRNA-mRNA interactions. *Mol. Biol. Cell* **24**, 1638-1648.

Keppeke, G. D., Nunes, E., Ferraz, M. L. G., Silva, E. A. B., Granato, C., Chan, E. K. L. and Andrade, L. E. C. (2012). Longitudinal study of a human drug-induced model of autoantibody to cytoplasmic rods/rings following HCV therapy with ribavirin and interferon-alpha. *PLoS ONE* **7**, e45392.

Keppeke, G. D., Satoh, M., Ferraz, M. L., Chan, E. K. and Andrade, L. E. (2014). Temporal evolution of human autoantibody response to cytoplasmic rods and rings structure during anti-HCV therapy with ribavirin and interferon-alpha. *Immunol. Res.* **60**, 38-49.

Keppeke, G. D., Calise, S. J., Chan, E. K. L. and Andrade, L. E. C. (2015). Assembly of IMPDH2-based, CTPS-based, and mixed rod/ring structures is dependent on cell type and conditions of induction. *J. Genet. Genomics* **42**, 287-299.

Kim, D., Fiske, B. P., Birsoy, K., Freinkman, E., Kami, K., Possemato, R. L., Chudnovsky, Y., Pacold, M. E., Chen, W. W., Cantor, J. R. et al. (2015). SHMT2 drives glioma cell survival in ischaemia but imposes a dependence on glycine clearance. *Nature* **520**, 363-367.

Kristofferson, D. and Purich, D. L. (1981). Time scale of microtubule length redistribution. *Arch. Biochem. Biophys.* **211**, 222-226.

Lian, S. L., Li, S., Abadal, G. X., Pauley, B. A., Fritzler, M. J. and Chan, E. K. L. (2009). The C-terminal half of human Ago2 binds to multiple GW-rich regions of GW182 and requires GW182 to mediate silencing. *RNA* **15**, 804-813.

Liu, J.-L. (2010). Intracellular compartmentation of CTP synthase in Drosophila. *J. Genet. Genomics* **37**, 281-296.

Nair, V. and Shu, Q. (2007). Inosine monophosphate dehydrogenase as a probe in antiviral drug discovery. *Antivir. Chem. Chemother.* **18**, 245-258.

Narkewicz, M. R., Sauls, S. D., Tjoa, S. S., Teng, C. and Fennessey, P. V. (1996). Evidence for intracellular partitioning of serine and glycine metabolism in Chinese hamster ovary cells. *Biochem. J.* **313**, 991-996.

Noree, C., Sato, B. K., Broyer, R. M. and Wilhelm, J. E. (2010). Identification of novel filament-forming proteins in Saccharomyces cerevisiae and Drosophila melanogaster. *J. Cell Biol.* **190**, 541-551.

O'Connell, J. D., Zhao, A., Ellington, A. D. and Marcotte, E. M. (2012). Dynamic reorganization of metabolic enzymes into intracellular bodies. *Annu. Rev. Cell Dev. Biol.* **28**, 89-111.

Purich, D. L. (2010). Enzyme kinetics: catalysis & control : a reference of theory and best-practice methods. San Diego, Calif; Oxford: Elsevier Academic; Elsevier Science distributor.

Ratcliffe, A. J. (2006). Inosine 5′-monophosphate dehydrogenase inhibitors for the treatment of autoimmune diseases. *Curr. Opin. Drug Discov. Dev.* **9**, 595-605.

Schindelin, J., Arganda-Carreras, I., Frise, E., Kaynig, V., Longair, M., Pietzsch, T., Preibisch, S., Rueden, C., Saalfeld, S., Schmid, B. et al. (2012). Fiji: an open-source platform for biological-image analysis. *Nat. Methods* **9**, 676-682.

Shu, Q. and Nair, V. (2008). Inosine monophosphate dehydrogenase (IMPDH) as a target in drug discovery. *Med. Res. Rev.* **28**, 219-232.

Stover, P. and Schirch, V. (1990). Serine hydroxymethyltransferase catalyzes the hydrolysis of 5,10-methenyltetrahydrofolate to 5-formyltetrahydrofolate. *J. Biol. Chem.* **265**, 14227-14233.

Stover, P. and Schirch, V. (1993). The metabolic role of leucovorin. *Trends Biochem. Sci.* **18**, 102-106.

Thomas, E. C., Gunter, J. H., Webster, J. A., Schieber, N. L., Oorschot, V., Parton, R. G. and Whitehead, J. P. (2012). Different characteristics and nucleotide binding properties of inosine monophosphate dehydrogenase (IMPDH) isoforms. *PLoS ONE* **7**, e51096.

Weber, G. (1983). Biochemical strategy of cancer cells and the design of chemotherapy: G. H. A. Clowes Memorial Lecture. *Cancer Res.* **43**, 3466-3492.

Yao, B., Li, S., Jung, H. M., Lian, S. L., Abadal, G. X., Han, F., Fritzler, M. J. and Chan, E. K. L. (2011). Divergent GW182 functional domains in the regulation of translational silencing. *Nucleic Acids Res.* **39**, 2534-2547.

Yao, B., La, L. B., Chen, Y. C., Chang, L. J. and Chan, E. K. (2012). Defining a new role of GW182 in maintaining miRNA stability. *EMBO Rep.* **13**, 1102-1108.

Zhao, H., French, J. B., Fang, Y. and Benkovic, S. J. (2013). The purinosome, a multi-protein complex involved in the de novo biosynthesis of purines in humans. *Chem. Commun.* **49**, 4444-4452.

Zhao, H., Chiaro, C. R., Zhang, L., Smith, P. B., Chan, C. Y., Pedley, A. M., Pugh, R. J., French, J. B., Patterson, A. D. and Benkovic, S. J. (2015). Quantitative analysis of purine nucleotides indicates that purinosomes increase de novo purine biosynthesis. *J. Biol. Chem.* **290**, 6705-6713.